Structural Engineering and Mechanics, *Vol. 73, No. 1 (2020) 75-82*
DOI: https://doi.org/10.12989/sem.2020.73.1.075

Torsion of circular open cross-section with corrugated inner and outer surface

Yaşar Pala[1] and Abdullah Pala*[2]

[1]*Uludag University, Engineering Faculty, Gorukle 16059, Bursa-Turkey*
[2]*Bursa Technical University, Engineering Faculty, Department of Mechatronics, Bursa-Turkey*

(Received May 21, 2019, Revised August 26, 2019, Accepted September 5, 2019)

Abstract. In this study, the problem of torsion of bars with open cross section surrounded by corrugated boundaries is analyzed. An approximate analytical solution is given using perturbation technique. First, the stress analysis for circular open cross-section for arbitrary opening angle is formulated and the problem is analytically solved. Second, the open cross-section with corrugated cross section is analyzed using perturbation method. First order contributions to the stresses and the torques have been added. The results have been exemplified and compared by considering special examples.

Keywords: torsion, circular, open cross section, corrugated surface, stress, perturbation

1. Introduction

The problem of torsion of bars of solid or open cross-sections is an old, but important topic in structural engineering since applied torques render the members to fail. Therefore, the torsion of prismatic bars with solid, closed and open cross-sections has been extensively investigated in the literature (Timoshenko and Goodier 1956). Exact and approximate solutions have been found for various solid cross-sectional shapes using the method of separation of variables, direct integration method, conformal mapping and semi-inverse method (Timoshenko and Goodier 1956, Rekach 1977, Venkatraman and Patel 1970). On the same line, the torsion of cylindrical bars with corrugated surface has also been studied Wang (Wang 1994). In recent years, especially, thin walled steel sections subjected to twisting moments have received great attention since they are prone to large angles of twist. Closed form solutions for the torsional analysis of thin-walled beams under various loads and boundary conditions were presented in many papers (Seaburg and Carter 1997, Barsoum and Gallagher 1970, Erkmen and Mohareb 2006) and vice versa. The elastic-plastic fracture of functionally graded circular shafts in torsion has been investigated by Rizov (Rizov 2016). Strength case of pre-stressed concrete beams in torsion has been investigated by Karayannis and Chalioris (Karayannis and Chalioris 2010). Mazloom, *et al*.2015, studied the compressive, shear and torsional strength of beams made of self-compacting concrete. Yoon *et al* (2017), investigated non-linear torsional analysis of 3D composite beams using the extended St. Venant solution. Taborda *et al.* (2018), studied the effective torsional strength of axially restricted RC beams.

Nguyen et *al*. (2018), studied the buckling analysis of an axially loaded thin-walled open-section beam with functionally graded materials. The latest works on the subject are rather based on finite element formulation. However, the torsion of some open cross-sections can still be examined via analytical methods and judiciously produced handy formulae can be presented for everyday usage. The results can also be compared with those available in the literature. Such a practically important problem is depicted in Figs. 1(a), (b). In the present paper, first, the analysis of a bar with open circular cross-section twisted by the applied torque is to be proceeded. Second, the stress analysis of a bar of the cross-section with corrugated surfaces under twisting moments is examined.

1.1 *Theory and analysis*

In order to find the governing equation, let us consider a solid cylindrical bar with an arbitrary cross-section. The bar is assumed to undergo a twisting moment applied at the end planes in Fig. (1). According to the displacement approach, it is assumed that the displacement components of the problem are proposed in the forms

$$u = -\alpha yz, \quad v = \alpha xz, \quad w = \alpha\psi(x, y) \tag{1}$$

where u, v correspond to x and y axes and Ψ is a called the warping function. Accordingly, strain-displacement relations and nonzero shear stresses are shown to be

$$\gamma_{yz} = \alpha\left(\frac{\partial\psi}{\partial y} + x\right), \quad \gamma_{xz} = \alpha\left(\frac{\partial\psi}{\partial x} - y\right) \tag{2a}$$

and

*Corresponding author, Professor
E-mail: mypala@uludag.edu.tr
[a] M.Sc. Candidate
E-mail: Abdulla_pala2011@hotmail.com

ISSN: 1225-4568 (Print), 1598-6217 (Online)

$$\tau_{yz} = G\alpha\left(\frac{\partial\psi}{\partial y} + x\right), \quad \tau_{xz} = G\alpha\left(\frac{\partial\psi}{\partial x} - y\right) \tag{2b}$$

If Eqs. (2b) are used in the stress-equilibrium equations, one obtains

$$\nabla^2\psi = 0 \tag{3}$$

On the other hand, if it is assumed that the stresses are derivable from a stress function ϕ such that

$$\tau_{yz} = -\frac{\partial\phi}{\partial x}, \quad \tau_{xz} = \frac{\partial\phi}{\partial y} \tag{4}$$

The equilibrium relation is satisfied. Taking

$$\gamma_{yz} = -\frac{1}{G}\frac{\partial\phi}{\partial x}, \quad \gamma_{xz} = \frac{1}{G}\frac{\partial\phi}{\partial y} \tag{5}$$

and putting into Eq.(2), one finds

$$\nabla^2\phi = -2\alpha G \tag{6}$$

Eq.(6) is to be solved under the boundary condition $\phi=0$. In the present study, after solving the first part of the problem, we obtain the approximate analytical solution for the cross-section of corrugated boundaries using perturbation method.

In the case of corrugated surfaces, the inner and outer boundaries are assumed to have corrugation defined by

$$\begin{aligned} &\text{(Inner)} && r_1 = a + h\varepsilon\sin(i\theta) = a + h\varepsilon S \\ &\text{(Outher)} && r_2 = b + l\varepsilon\sin(m\theta + \varphi) = b + l\varepsilon\bar{S} \end{aligned} \tag{7}$$

Here, i, m are integers, φ is the phase shift, a, b are the inner and outher radii, h, l are non-negative numbers and ε is a small number. These corrugations may be imprecise machining or may be intentional.

In terms of Prandtl stress function ϕ, the torsion problem is defined as

$$\nabla^2\phi = -2\alpha G \tag{8}$$

$$\phi = 0, \quad on\ C\ ; \quad \phi = 0, \quad \text{on } D$$

$$\phi = 0, \quad on\ A\ ; \quad \phi = 0, \quad \text{on } B$$

where G is the shear modulus of elasticity, α is the angle of twist per unit length. Recall that the stress function is zero both on the inner and outer boundary since the region is simply connected.

1.2 The case of circular open cross-section

The poisson equation (Eq.8) must be solved such that the stress function ϕ is zero on the boundaries A,B,C and D. In order to find an explicit solution satisfying Eq.(8) and the stress function ϕ must have the form

$$\phi(r,\theta) = \sum_{n=0}^{\infty} f_n(r)\sin(\beta\theta), \qquad \beta = \frac{2n+1}{k} \tag{9}$$

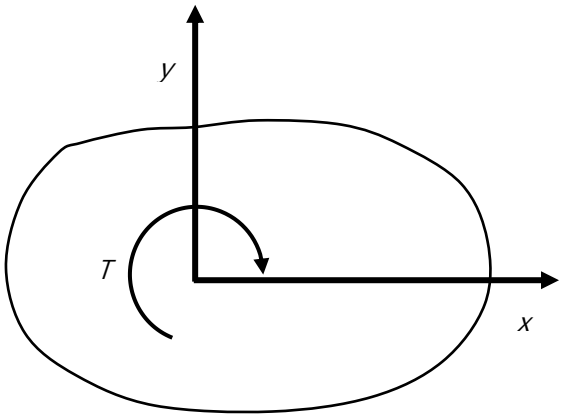

Fig. 1 A Bar of non-circular cross-section subjected to twisting moment T

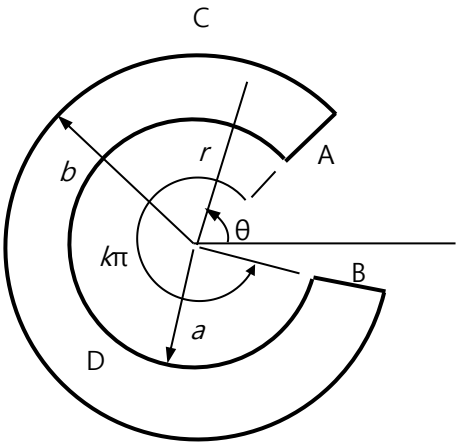

(a)

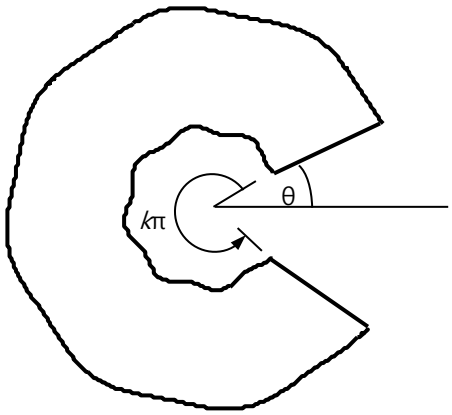

(b)

Fig. 2 a) Open circular cross-section b) Open corrugated cross-section

where k is a real number. Recall that the boundary conditions on A and B are automatically satisfied by Eq. (9). We expand the right –hand side of the Eq. (8) in the interval $0 \le \theta < k\pi$ into Fourier sinus series

$$-2\alpha G = \frac{-8\alpha G}{\pi}\sum_{n=0}^{\infty}\frac{1}{2n+1}\sin(\beta\theta), \tag{10}$$

Substituting Eqs. (9) and (10) into Eq. (8) yields

$$\frac{d^2 f_n}{dr^2}+\frac{1}{r}\frac{df_n}{dr}-\frac{\beta^2}{r^2}f_n=\frac{-8\alpha G}{\pi(2n+1)} \tag{11}$$

Here, the form of Laplace operator ∇^2 in polar coordinates is used. It can be readily shown that the homogenous solution $(f_n(r))_h$ and the proper solution $(f_n)_p$ of Eq.(11) are given by

$$f_n(r)=A_n r^{\beta}+B_n r^{-\beta}, \qquad (f_n(r))_p=C_n r^2 \tag{12}$$

where A_n, B_n are undetermined constants and C_n is given by

$$C_n=\frac{-8\alpha G}{\pi(2n+1)}\frac{1}{(2-\beta)(2+\beta)}, \tag{13}$$

Hence, the general solution of Eq.(11) is written

$$f_n(r)=A_n r^{\beta}+B_n r^{-\beta}+C_n r^2 \tag{14}$$

In order to obtain the values of A_n, B_n, recall that the boundary conditions $\phi\big|_{r=a}=0$ and $\phi\big|_{r=b}=0$ require that $f_n(a)=0$ and $f_n(b)=0$. Using these conditions in Eq. (14) yield

$$A_n=\frac{a^{2-\beta}\left[\left(\frac{b}{a}\right)^{2+\beta}-1\right]}{\left[1-\left(\frac{b}{a}\right)^{2\beta}\right]}C_n, \qquad B_n=\frac{a^2 b^{\beta}\left[\left(\frac{b}{a}\right)^{\beta}-\left(\frac{b}{a}\right)^{2}\right]}{\left[1-\left(\frac{b}{a}\right)^{2\beta}\right]}C_n \tag{15}$$

Substituting Eq.(14) into Eq.(9) , we have

$$\phi_0(r,\theta)=\sum_{n=0}^{\infty}\left(A_n r^{\beta}+B_n r^{-\beta}+C_n r^2\right)\sin(\beta\theta), \tag{16}$$

Stresses $\tau_{z\theta}$ and τ_{zr} can be written as

$$\tau_{z\theta}=-\frac{\partial\phi}{\partial r}=-\left[\sum_{n=0}^{\infty}\left(A_n\beta r^{\beta}+\beta B_n r^{-\beta}+2C_n\beta r\right)\cos(\beta\theta)\right] \tag{17}$$

and

$$\tau_{zr}=\frac{1}{r}\frac{\partial\phi}{\partial\theta}=\frac{1}{r}\left[\sum_{n=0}^{\infty}\left(A_n r^{\beta}+B_n r^{-\beta}+C_n r^2\right)\beta\cos(\beta\theta)\right] \tag{18}$$

respectively. Using Eq.(16), twisting moment is obtained as

$$M_z=2\iint_{R_A}\phi dxdy=2\iint_{R_A}\phi r dr d\theta$$
$$=2\sum_{n=0}^{\infty}\int_{r=a}^{r=b}\int_{\theta=0}^{\theta=k\pi}\left(A_n r^{\beta}+B_n r^{-\beta}+C_n r^2\right)\sin(\beta\theta) r dr d\theta \tag{19a}$$

or

$$M_z=\sum_{n=0}^{\infty}\frac{4}{\beta}\left\{\begin{array}{l}\frac{A_n}{2+\beta}\left(b^{2+\beta}-a^{2+\beta}\right)+\\ \frac{B_n}{2-\beta}\left(b^{2-\beta}-a^{2-\beta}\right)+\frac{C_n}{4}\left(\left(b^4-a^4\right)\right)\end{array}\right] \tag{19b}$$

Considering the expressions for A_n, B_n, C_n and factoring α in Eq.(19b), the unit angle of twist α can be written as

$$\alpha=\frac{M_z}{\bar{M}_z}=\frac{M_z}{\bar{M}_z/\alpha} \tag{20}$$

Here, $\bar{M}_z$ is obtained by factoring α from Eq.(19b).

The variation $M_z/G\alpha$ with the ratio b/a have been plotted in Figs.3-8 for various values of k's and a's. The number of n in all series below was taken $n = 40$. This figure is enough for the series to converge. It is obvious that $M_z/G\alpha$ increases with increasing values of the thickness and the inner radius a. As expected, $M_z/G\alpha$ also increases for increasing values of k. In fact, the increase in $k(0\le k\le 2)$ or the ratio b/a corresponds to increase in the area of the cross-section. Therefore, the increase in the ratio 0 $M_z/G\alpha$ is expectable.

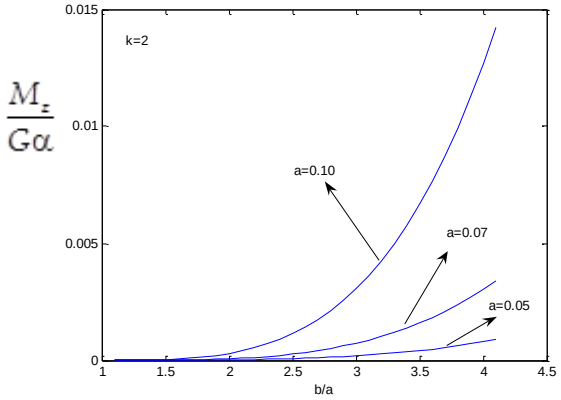

Fig. 3 The variation of $M_z/G\alpha$ with b/a for various values of a in the case of circular open cross section: $k = 2$

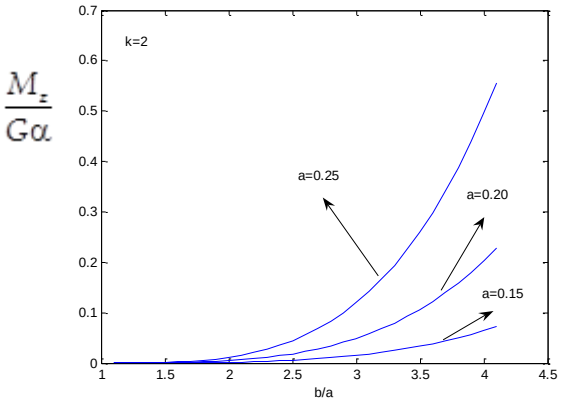

Fig. 4 The variation of $M_z/G\alpha$ with b/a for various values of a in the case of circular open cross section: $k = 2$

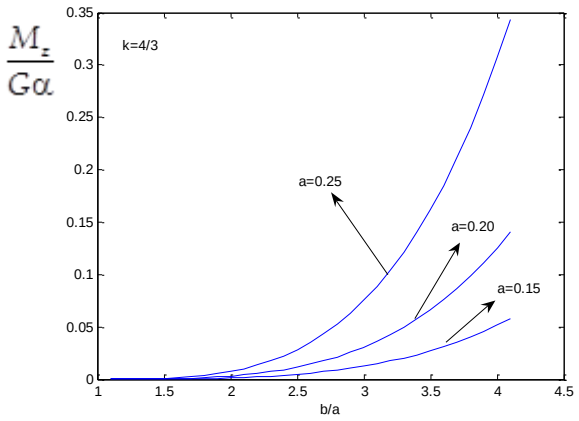

Fig. 5 The variation of $M_z/G\alpha$ with b/a for various values of a in the case of circular open cross section: $k = 4/3$

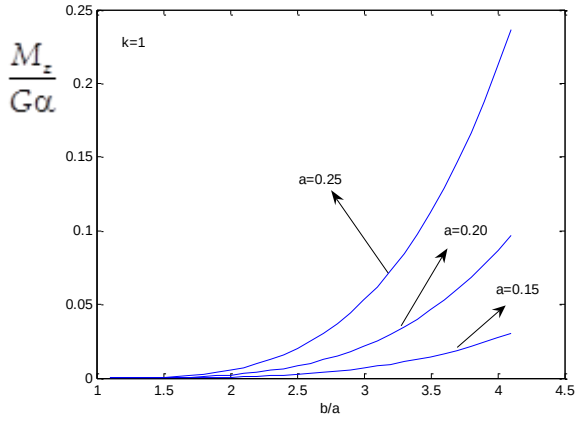

Fig. 6 The variation of $M_z/G\alpha$ with b/a for various values of a in the case of circular open cross section: $k = 1$

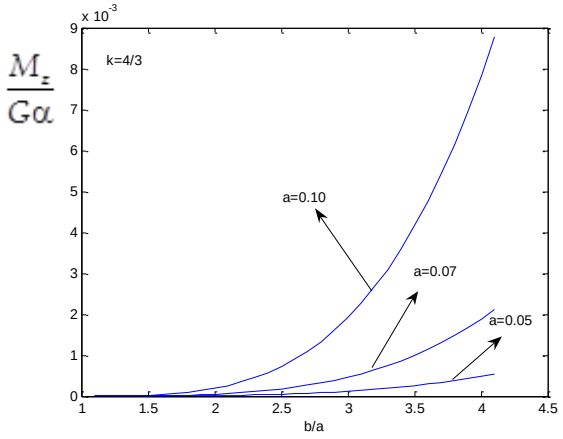

Fig. 7 The variation of $M_z/G\alpha$ with b/a for various values of a in the case of circular open cross section: $k = 4/3$

Figs. (9) and (10) show the variations of $\tau_{z\theta}/G\alpha$ $\tau_{z\theta}/G\alpha$ with the angle θ for various values of the inner radius a's and k's at the inner surface of the cylinder. $\tau_{z\theta}/G\alpha$ obviously increases with decreasing values of k and a. It is clear that $\tau_{z\theta}/G\alpha$ becomes zero at the angles θ=0 and $\theta=k\pi$. In Figs.(11) and (12), $\tau_{zr}/G\alpha$ versus θ is plotted for different values of a's and the thickness t. $\tau_{zr}/G\alpha$ obviously increases with decreasing value of a while it increases with increasing value of the t.

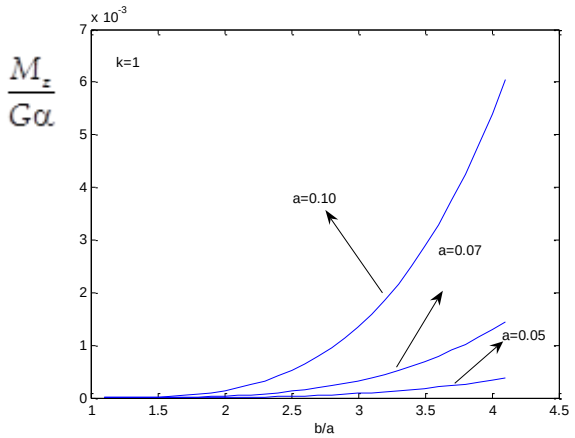

Fig. 8 The variation of M_z with b/a for various values of1 a in the case of circular open cross section: $k = 1$

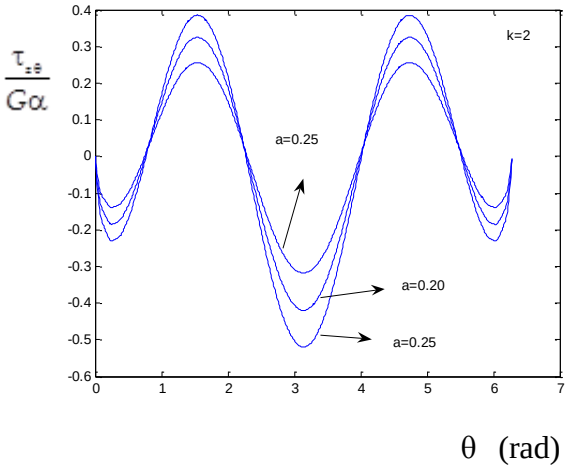

Fig. 9 The variation of $\tau_{z\theta}/G\alpha$ with the angle θ for various values of a in the case of circular open cross section: $r = a$, $k = 2$

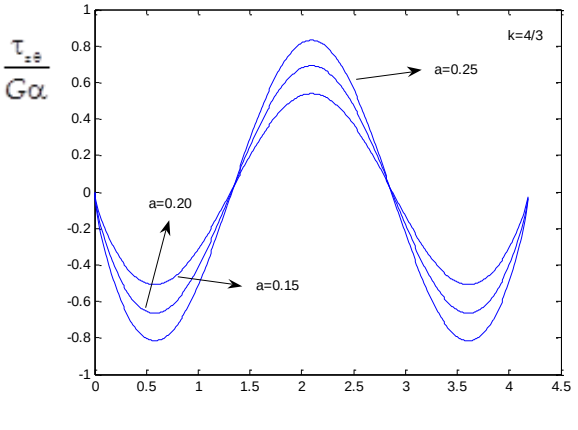

Fig. 10 The variation of $\tau_{z\theta}/G\alpha$ with the angle θ for various values of a in the case of circular open cross section: $r = a$, $k = 4/3$

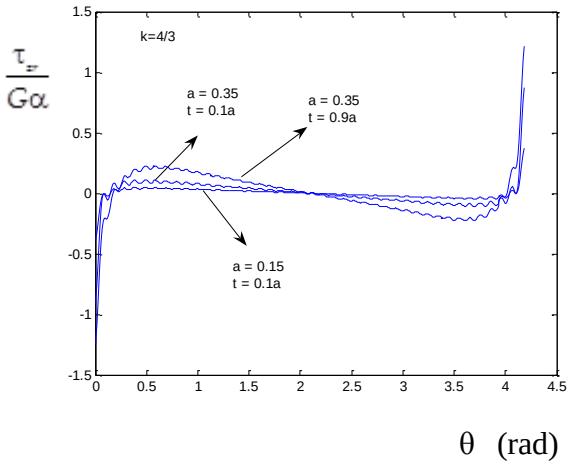

Fig. 11 The variation of $\tau_{zr}/G\alpha$ with the angle θ for various values of a and the thickness t in the case of circular open cross section: $r = a$, $k = 4/3$

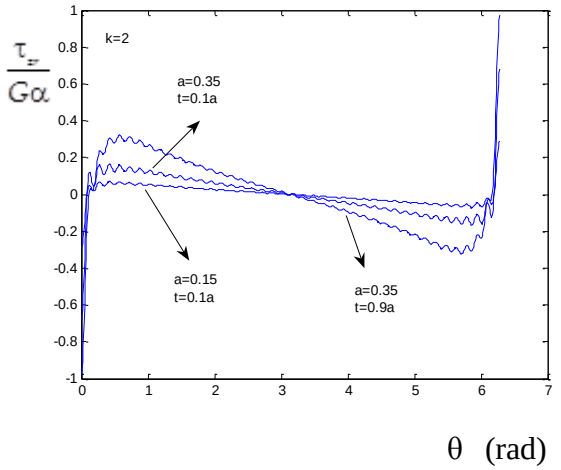

Fig. 12 The variation of $\tau_{zr}/G\alpha$ with the angle θ for various values of a and the thickness t in the case of circular open cross section: $r = a$, $k = 2$

1.3 The case of corrugated boundary surface

In this case, assuming small values for $h\varepsilon$ and $l\varepsilon$, we can expand the stress function $\phi(r,\theta)$ into a perturbation series as

$$\phi(r,\theta) = \phi_0(r,\theta) + \varepsilon\phi_1(r,\theta) + \varepsilon^2\phi_2(r,\theta) + \ldots \quad (21)$$

Substituting Eq. (21) into Eq.(8) yields a set of partial differential equations in the following forms:

$$\nabla^2\phi_0 = 2G\alpha, \quad (22a)$$

$$\nabla^2\phi_1 = 0, \quad (22b)$$

$$\nabla^2\phi_2 = 0, \quad \ldots \quad (22c)$$

Here, ϕ_0 is the stress function corresponding to the case of circular open cross-section whose analysis has been carried out in Section.1.1.

Since the stress function is still zero on the corrugated boundaries, we can write

$$\phi\big|_{r=a+h\varepsilon S} = 0 \quad \text{and} \quad \phi\big|_{r=b+l\varepsilon\bar{S}} = 0 \quad (23)$$

The stress function can be expanded into Taylor series around the points $r_1=a$ and $r_2=b$, respectively:

$$0 = \phi\big|_{r=a+h\varepsilon S} = \phi\big|_{r=a} + h\varepsilon S\frac{\partial\phi}{\partial r}\bigg|_a + \frac{h^2\varepsilon^2S^2}{2!}\frac{\partial^2\phi}{\partial r^2}\bigg|_a + \ldots \quad (24)$$

and

$$0 = \phi\big|_{r=b+l\varepsilon\bar{S}} = \phi\big|_{r=b} + l\varepsilon\bar{S}\frac{\partial\phi}{\partial r}\bigg|_b + \frac{l^2\varepsilon^3\bar{S}^2}{2!}\frac{\partial^2\phi}{\partial r^2}\bigg|_b + \ldots \quad (25)$$

Inserting Eq. (21) into Eqs. (24) and (25) and rearranging terms give

$$0 = \phi\big|_{r=a} + \varepsilon\left[\phi_1(a,\theta) + hS\phi_{0r}(a,\theta) + \ldots\right] + \varepsilon^2\left[\phi_2(a,\theta) + hS\phi_{1r}(a,\theta) + \frac{1}{2}h^2S^2\phi_{0rr}(a,\theta) + \ldots\right] + \ldots \quad (26)$$

and

$$0 = \phi\big|_{r=b} + \varepsilon\left[\phi_1(b,\theta) + l\bar{S}\phi_{0r}(b,\theta) + \ldots\right] + \varepsilon^2\left[\phi_2(b,\theta) + l\bar{S}\phi_{1r}(b,\theta) + \frac{1}{2}l^2\bar{S}^2\phi_{0rr}(b,\theta) + \ldots\right] + \ldots \quad (27)$$

In order that Eqs. (26) and (27) become valid for arbitrary values of ε, we must have

$$\phi_1(a,\theta) = -hS\frac{\partial\phi_0}{\partial r}(a,\theta) \quad (28a)$$

$$\phi_2(a,\theta) = -hS\frac{\partial\phi_1}{\partial r}(a,\theta) - \frac{1}{2}h^2S^2\frac{\partial^2\phi_0}{\partial r^2}(a,\theta) \quad (28b)$$

and

$$\phi_1(b,\theta) = -l\bar{S}\frac{\partial\phi_0}{\partial r}(b,\theta) \quad (29a)$$

$$\phi_2(b,\theta) = -l\bar{S}\frac{\partial\phi_1}{\partial r}(b,\theta) - \frac{1}{2}l^2\bar{S}^2\frac{\partial^2\phi_0}{\partial r^2}(b,\theta) \quad (29b)$$

Two sets given by Eqs. (28) and Eqs.(29) are the boundary conditions for $\phi_1,\phi_2,\phi_3,\ldots$ at the inner and outer boundaries, respectively.

In order to determine $\phi_1(r,\theta)$, we must seek the solution of Eq.(22b) subjected to the conditions Eqs.(28a) and (29a). Substituting the expressions for $\phi_0(a,\theta)$ into Eq.(28a) and Eq.(29a), we obtain

$$\phi_1(a,\theta) = -hS\sum_{n=0}^{\infty}\left(\beta A_n a^{\beta-1} - \beta B_n a^{-\beta-1} + 2C_n a\right)\sin(\beta\theta) = \gamma_0\sin(\beta\theta), \quad (30)$$

and

$$\phi_1(b,\theta) = -l\bar{S}\sum_{n=0}^{\infty}\left(\beta A_n b^{\beta-1} - \beta B_n b^{-\beta-1} + 2C_n b\right)\sin(\beta\theta) = \varsigma_0\sin(\beta\theta), \quad (31)$$

where γ_0 and ς_0 are defined by

$$\gamma_0 = -hS\sum_{n=0}^{\infty}\left(\beta A_n a^{\beta-1} - \beta B_n a^{-\beta-1} + 2C_n a\right) \quad (32)$$

$$\varsigma_0 = -lS\sum_{n=0}^{\infty}\left(\beta A_n b^{\beta-1} - \beta B_n b^{-\beta-1} + 2C_n b\right) \quad (33)$$

Taking the forms of boundary values into account, we seek the approximate analytical solution of Eq.(22b) in the form

$$\phi_1(r,\theta) = \sum_{n=0}^{\infty} g_n(r)\sin(\beta\theta), \qquad \beta = \frac{2n+1}{k} \quad (34)$$

Recall that Eq. (34) also satisfies the condition of $\phi_1(r,0)=0$ and $\phi_1(r,k\pi)=0$. Inserting Eq.(34) into Eq.(22b) yields

$$\frac{d^2 g_n}{dr^2} + \frac{1}{r}\frac{dg_n}{dr} - \frac{\beta^2}{r^2} g_n = 0 \quad (35)$$

The form of Eq.(35) is the same as with the left side of Eq.(11). Hence, the solution has the form

$$g_n(r) = \bar{A}_n r^{\beta} + \bar{B}_n r^{-\beta}, \quad (36)$$

where $\bar{A}_n$, $\bar{B}_n$ are yet to be determined. Comparing Eq.(34) and the boundary conditions on $\phi_1(r,\theta)$ given by Eqs.(28a),(29a) , we conclude that the boundary conditions on $g_n(r)$ must be

$$g_n(a) = \gamma_0 \quad (37)$$

$$g_n(b) = \varsigma_0 \quad (38)$$

Using Eqs.(36), (37) and (38) , $\bar{A}_n$, $\bar{B}_n$ are obtained as

$$\bar{A}_n = \gamma_0 a^{-\beta} - a^{-2\beta}\left(\frac{\left(\gamma_0 a^{-\beta} - \varsigma_0 b^{-\beta}\right)}{a^{-2\beta} - b^{-2\beta}}\right) \quad (39)$$

$$\bar{B}_n = \frac{\left(\varsigma_0 a^{-\beta} - \gamma_0 b^{-\beta}\right)}{\left(a^{-2\beta} - b^{-2\beta}\right)} \quad (40)$$

Now, $\phi_1(r,\theta)$ is written as

$$\phi_1(r,\theta) = \sum_{n=0}^{\infty}\left(\bar{A}_n r^{\beta} + \bar{B}_n r^{-\beta}\right)\sin(\beta\theta), \quad 0 \le \theta < k\pi \quad (41)$$

Inserting Eqs. (16) and (41) into Eq.(21) , we finally obtain

$$\phi(r,\theta) = \phi_0 + \varepsilon\phi_1 = \sum_{n=0}^{\infty}\left((A_n + \varepsilon\bar{A}_n)r^{\beta} + (B_n + \varepsilon\bar{B}_n)r^{-\beta}\right)\sin(\beta\theta), \quad 0 \le \theta < k\pi \quad (42)$$

Here, only first order terms have been kept, and higher order terms have been omitted. Stresses $\tau_{z\theta}$ and τ_{zr} in the present case can be written as

$$\tau_{z\theta} = -\frac{\partial\phi}{\partial r} = -\sum_{n=0}^{\infty}\begin{pmatrix}\left(A_n + \varepsilon\bar{A}_n\right)\beta r^{\beta-1} \\ -\beta\left(B_n + \varepsilon\bar{B}_n\right)r^{-\beta-1} + 2C_n r\end{pmatrix}\sin(\beta\theta) \quad (43)$$

and

$$\tau_{zr} = \frac{1}{r}\frac{\partial\phi}{\partial\theta} = \left[\frac{1}{r}\sum_{n=0}^{\infty}\begin{pmatrix}\left(A_n + \varepsilon\bar{A}_n\right)r^{\beta} \\ +\left(B_n + \varepsilon\bar{B}_n\right)r^{-\beta} + C_n r^2\end{pmatrix}\beta\cos(\beta\theta)\right] \quad (44)$$

Utilizing Eq.(19) for the resultant applied torque over the solid cross-section and Eq.(42) , we obtain

$$M_z = \sum_{n=0}^{\infty}\frac{4}{\beta}\left\{\begin{bmatrix}\frac{A_s}{1+\beta}\left(b^{2+\beta} - a^{2+\beta}\right) \\ +\frac{B_s}{1-\beta}\left(b^{2-\beta} - a^{2-\beta}\right) + \frac{C_n}{4}\left(\left(b^4 - a^4\right)\right)\end{bmatrix}\right. \quad (45)$$

Here, A_s and B_s are given by

$$A_s = A_n + \varepsilon\bar{A}_n, \; B_s = B_n + \varepsilon\bar{B}_n \quad (46)$$

The variations of $\tau_{z\theta}/G\alpha$ with the angle θ at the inner surface of the cross section are plotted in Figs. 13,14,15,16 and (17) for various values of the parameters. The influence of the corrugation is depicted on each figure. The number of n was again taken n = 40 in calculating the series. Figs.(13) and (14) show the comparison of stresses $\tau_{z\theta}/G\alpha$ between the corrugated and un-corrugated surfaces. These figures reveal that $\tau_{z\theta}/G\alpha$ increases with decreasing value of a's. We also observe that the peak values of the stress $\tau_{z\theta}/G\alpha$ decreases with increasing values of k's. $\tau_{z\theta}/G\alpha$ is influenced little by the value of ε, as seen in Figs.(15) and (16). However, for larger values of ε, the corrugation can influence the stresses at an appreciable rate. Figs.(18), (19) depict the variation of $\tau_{zr}/G\alpha$ with the angle θ at the inner surface for various values of the variables. The stress values increase for increasing values of a's. It is clear that the stresses decrease with corrugation.

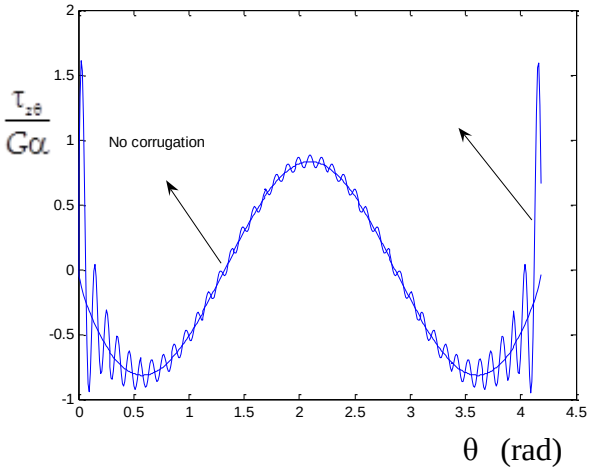

Fig. 13 The variation of $\tau_{z\theta}/G\alpha$ with the angle θ: a=0.25, t = 0.1a, hS = 0.05, lS = 0.05, k = 4/3, r = a

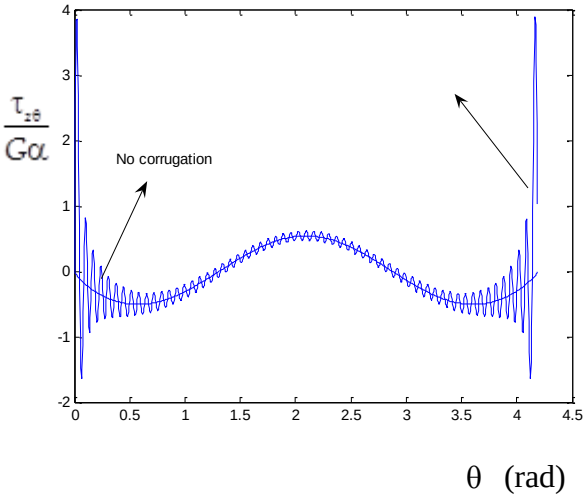

Fig. 14 The variation of $\tau_{z\theta}/G\alpha$ with the angle θ: $a = 0.15$, $t = 0.1a$, $hS = 0.05$, $lS = 0.05$, $k = 4/3$, $r = a$

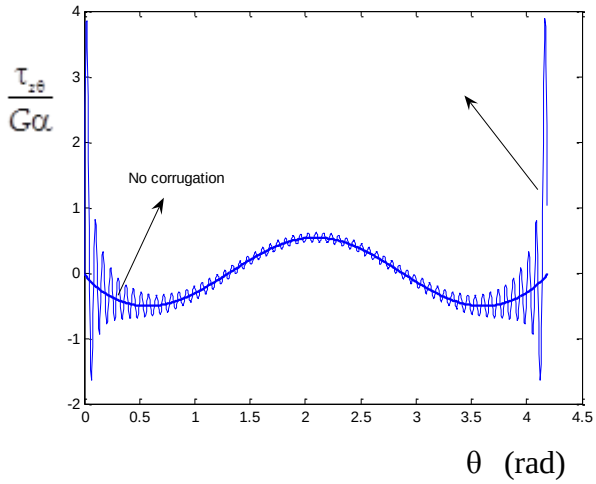

Fig. 15 The variation of $\tau_{z\theta}/G\alpha$ with the angle θ: $a = 0.15$, $t = 0.1a$, $hS = 0.05$, lS = 0.05 , $k = 4/3$, $r = a$

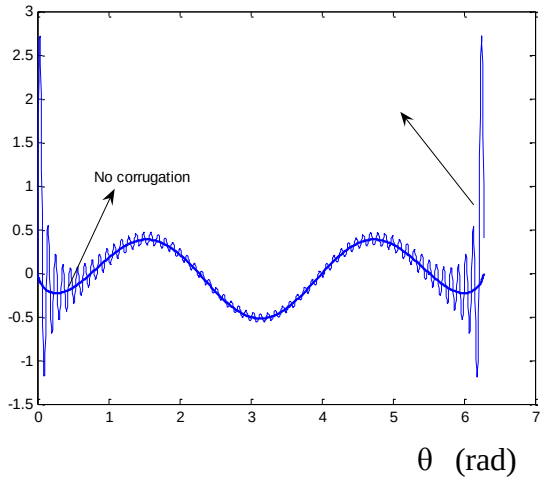

Fig. 16 The variation of $\tau_{z\theta}/G\alpha$ with the angle θ: a=0.25, $t = 0.1a$, $hS = 0.05$, $lS = 0.05$, k=2, r=a

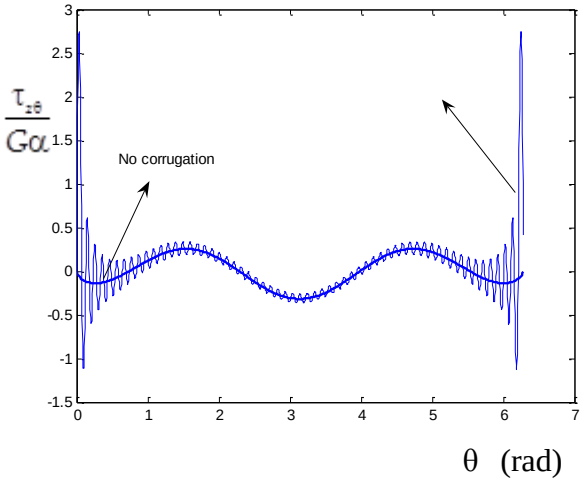

Fig. 17: The variation of $\tau_{z\theta}/G\alpha$ with the angle θ: $a = 0.15$, $t = 0.1a$, $hS = 0.05$, $lS = 0.05$, $k = 2$, $r = a$

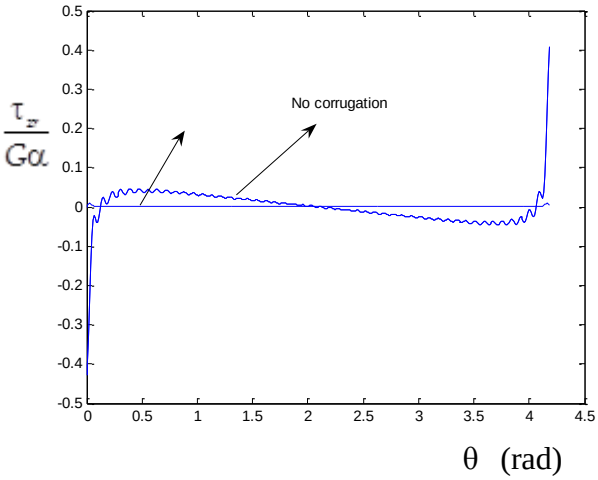

Fig. 18 The variation of $\tau_{zr}/G\alpha$ with the angle θ: $a = 0.15$, $t = 0.1a$, $hS = 0.05$, $lS = 0.05$, $k = 4/3$, $r = a$,

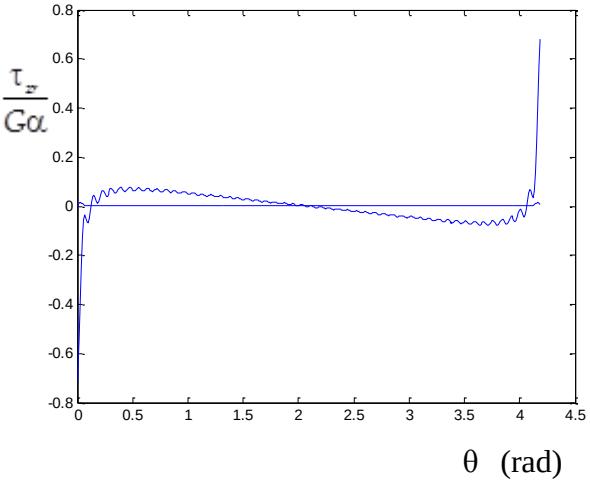

Fig. 19 The variation of $\tau_{zr}/G\alpha$ with the angle θ: $a = 0.25$, $t = 0.1a$, $hS = 0.05$, $lS = 0.05$, $k = 4/3$, $r = a$

2. Results and discussion

We have analyzed the stress distribution for the problem of torsion of a bar with the cross section of corrugated boundaries. To do with, first, the problem of open circular cross section has been solved. Later, first order contributions have been added to the solution using perturbation method. However, without having any difficulty, second order contributions can also be added to the solution. It is estimated that these second contributions will be of small value. The method developed has been applied on a specific example, and the effect of corrugation at the inner surface of the cross section has been observed. It has been observed that the stress values in the case of corrugated surfaces can appreciably be influenced by the corrugation and the values of variables. Since the analytical expressions have been obtained in the present work, every kind of effect can be observed by using the results of the present study. By changing the values hS, $l\bar{S}$, ε, i, m and φ, different types of practically important shapes can be obtained. By choosing the thickness too small, analytical results for the thin walled open cross-section under twisting moments can be obtained and readily compared with those of numerical methods. Using, for example, Eqs.(17) and (18) and recalling the relation $\tau = G\alpha r$ for the case of circular solid section, one can compare the present results with those of circular solid cross- section, and see the deviation of the results in the case of open cross-section. As a future work, it is estimated that the present analysis can possibly be applied to the axially loaded plates with a central hole of corrugated boundary.

References

Barsoum, R.S. and Gallagher, R.H. (1970), "A Finite element analysis of torsional and torsional-flexural stability problems", *Introduction J. Numerical Methods*, 335-352. https://doi.org/10.1002/nme.1620020304.

Erkmen, R.E. and Mohareb, M. (2006), "Torsion analysis of thin-walled beams including shear deformation effects", *Thin-Walled Struct.,* **44**, 1096-1108. https://doi.org/10.1016/j.tws.2006.10.012Get rights and content

Rekach, V.G. (1977), *Manual of The Theory of Elasticity*, 185-209, Mir Publishers, Moscow, Russia.

Seaburg, P.A. and Carter, J.C. (1997), *Torsional Analysis of Structural Steel Members*, American Institute of Steel Construction, (AISC), Chicago, IL, USA.

Timoshenko, S.P. and Goodier, J.N. (1956), *Theory of Elasticity*, Chapter 10, 291-323, McGraw-Hill, New York, USA.

Venkatraman, B. and Patel, S.A. (1970)*, Structural Mechanics with Introduction to Elasticity and Plasticity,* McGraw-Hill, New York, USA.

Wang, C.Y. (1994), "Torsion of a tube with longitudinal corrugations", *J. Appl. Mech.*, **61**(2), 489-491. https://doi.org/10.1115/1.2901478.

Rizov, V.I. (2016), "Elastic-plastic fracture of functionally graded circular shafts in torsion", *Adv. Mater. Res.*, **5**(4), 299-318. https://doi.org/10.12989/amr.2016.5.4.299.

Karayannis C.G. and Chalioris C.E. (2000), "Strength of prestressed concrete beams in torsion", *Struct. Eng. Mech.*, **10**(2),165-180. https://doi.org/10.12989/sem.2000.10.2.165.

Mazloom M, Saffari A. and Mehrvand M. (2015), "Compressive, shear and torsional strength of beams made of self-compacting concrete", *Comput. Concrete*, **15(**6), 935-950. https://doi.org/10.12989/cac.2015.15.6.935.

Yoon, K., D.Y., Kim and P.S., Lee. (2017), "Nonlinear torsional analysis of 3D composite beams using the extended St. Venant solution", *Struct. Eng. Mech.*, **62**(1), 33-42. https://doi.org/10.12989/sem.2017.62.1.033.

Taborda, C.S.B, Bernardo, L.F.A. and Gamma, J.M.R. (2018), "Gama Effective torsional strength of axially restricted RC beams", *Struct. Eng. Mech.*, **67**(5), 465-479. http://doi.org/10.12989/sem.2018.67.5.465.

Nguyen, T.T., Thang, P.T. and Lee, J. (2018), "Flexural-torsional stability of thin-walled functionally graded open-section beams", *Thin-Walled Struct.,* **110**,88-96. https://doi.org/10.1016/j.tws.2016.09.021.

PL